

EXPERIMENTAL VALIDATION OF THE CORBELLA'S VISIBILITY FUNCTION USING HUT-2D AND MIRAS

*F. Martin-Porqueras*¹, *J. Kainulainen*², *M. Martin-Neira*¹, *I. Corbella*³, *R. Oliva*¹, *R. Castro*⁴,
*J. Barbosa*⁴, and *A. Gutierrez*⁴

¹European Space Agency, ²Aalto University, ³Polytechnic University of Catalonia,
⁴Deimos Engenharia

ABSTRACT

The Corbella's revision of the fundamental equation of the interferometric aperture synthesis radiometry is verified using airborne and spaceborne data. This experimental verification uses the measurements of the airborne instrument HUT-2D from the Aalto University (Helsinki), and the unique spaceborne microwave imaging radiometer by aperture synthesis (MIRAS) from the ESA's Soil Moisture and Ocean Salinity (SMOS) mission. The data acquired with those sensors support the Corbella's revision of the visibility function. The revised function predicts that visibilities depend on the contrast between the target's brightness temperature and the backward noise of the receivers emitted through the antennas.

Index Terms— interferometry, microwave radiometry, visibility equation, MIRAS, aperture synthesis

1. INTRODUCTION

Soil Moisture and Ocean Salinity (SMOS) is the ESA's Earth Observation mission intended for the measurement of the sea surface salinity and soil moisture by means of the L-band surface emissivity [1][2].

The spatial resolution requirements for passive imaging at L-band lead to large antenna apertures [3] for which arrays using aperture synthesis principles offer clear advantages mechanically and electronically to steered antennas and push-broom radiometers.

Although two-dimensional aperture synthesis has been used in radio-astronomy for several decades, its application to a downward-looking sensor for Earth observation is new [4] [5] and SMOS is the first space mission boarding an L-band Microwave Imaging Radiometer by Aperture Synthesis (MIRAS). During the development, much has been learnt about two-dimensional aperture synthesis for Earth observation, and the results obtained with the airborne demonstrators and their calibration system thus far have demonstrated the technical feasibility of exploiting a spaceborne sensor of this type.

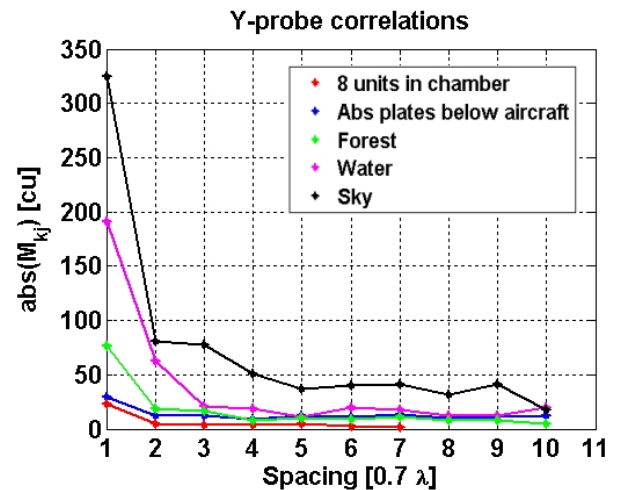


Fig. 1. Normalized visibilities measured by HUT-2D

The main contribution of SMOS to the microwave aperture synthesis interferometry is the link between the microwave theory and the radio-astronomy theory. Both theories have been linked by means of the modification in the visibility function proposed by Prof. Corbella [6] which predicts that visibilities measured by an aperture synthesis radiometer are dependent to the difference between the target's brightness temperature and the backward noise of the receivers emitted through the antennas.

The following sections present the experimental verification of the revised visibility function using HUT-2D and SMOS data. Special emphasis is done to the latter since it is the first spaceborne interferometric radiometer at L-band launched on November 2009.

2. VALIDATION USING AIRBORNE DATA

During the SMOS development, measurements acquired by AMIRAS (airborne MIRAS) [7] and HUT-2D [8] demonstrators have proved the validity of the visibility function proposed by Prof. Corbella. The method to experimentally validate the visibility function is measuring homogeneous targets since the visibility equation becomes directly proportional to the contrast between the brightness

TABLE I
TYPICAL BRIGHTNESS TEMPERATURE AT NADIR

Target	Value [K]
Anechoic chamber ceiling	290
Absorbent plates	290
Forest surface	250
Sea surface	100
Cold sky plus atmospheric contribution at zenith	7

temperature of the target and the backward noise of the receivers emitted through the antennas. The backward noise is equal to the receivers' physical temperature by design in AMIRAS, HUT-2D and MIRAS, since all the antennas include isolators.

In September 2004, MIRAS Demonstrator (AMIRAS precursor) measured the ceiling of an anechoic chamber and the cold sky [9], getting larger visibilities when imaging the Cold Sky as the Corbella's visibility function predicts.

AMIRAS results are extended by the validation conducted with HUT-2D using data acquired among several homogeneous targets. The selected targets cover the brightness temperature range from 7 to 290 K (Table 1). The measurements show a gradual increase with the contrast between the brightness temperature scene and the 295 K receivers' physical temperature. The comparison between the normalized visibilities for different targets is shown in Fig. 1. The normalized visibilities are expressed in correlation units (1 c.u = 1e-4) and the baseline spacing is 0.7 wavelengths.

3. VALIDATION USING IN-ORBIT SMOS DATA

After the successful launch of SMOS on November 2009, MIRAS is the most advanced microwave imaging radiometer at L-band. The instrument model is defined by the Corbella's visibility function. That model is product of the research conducted during the MIRAS development.

The instrument model was validated with engineering and airborne prototypes during the development phase. However, none of those prototypes reach the accuracy that MIRAS does.

Several activities intended to validate the Corbella's visibility function were planned to be conducted during the commissioning phase. This section presents the results of three of those validations.

3.1. Instrument physical temperature dependency

The thermal control system keeps the instrument physical temperature stable at 22 °C. However, the physical temperature was modified temporarily from 22 to 18 °C as part of the commissioning activities. That test was used to check the influence of the instrument physical temperature in the measurements as Corbella's revised visibility function predicted when observing the same region in the sky.

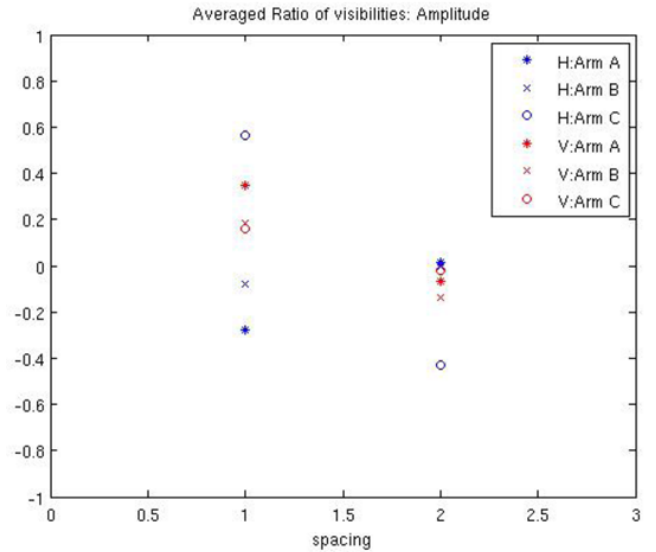


Fig. 2. Ratio between visibilities at 22 °C and 18 °C [dB]

The ratio between the average cold sky visibility at 22 (V₂₂) and 18 °C (V₁₈) has been computed (1). The ratio per each polarization and arm is shown in Fig. 2. The computation has been done for the 1 and 2-spacing baselines. In MIRAS, the baseline spacing is 0.875 wavelengths.

$$R = 10 \log \left(\left| \frac{\bar{V}_{22}}{\bar{V}_{18}} \right| \right) \quad (1)$$

The 1-spacing baselines are less affected by instrumental noise since they have higher signal to noise ratio. The results show that in average the magnitude of the cold sky visibilities in those particular baselines is higher when the instrument physical temperature is 22 °C. Therefore, those visibilities show an increase when the contrast between the brightness temperature scene and the receivers' physical temperature increases, as predicted by Corbella.

3.2. Flat Target Transformation

The Flat Target Transformation (FTT) is the processing algorithm which reduces the impact of the instrument errors, mainly induced by the antenna patterns uncertainties, in the image reconstruction [10].

The FTT minimizes the error in the brightness temperatures when the image reconstruction uses the transformed visibilities. According to the Corbella's visibility function, the visibilities are transformed subtracting them the 1 K instrument response (Flat Target Response) scaled by the contrast between the brightness temperature scene and the receivers' physical temperature.

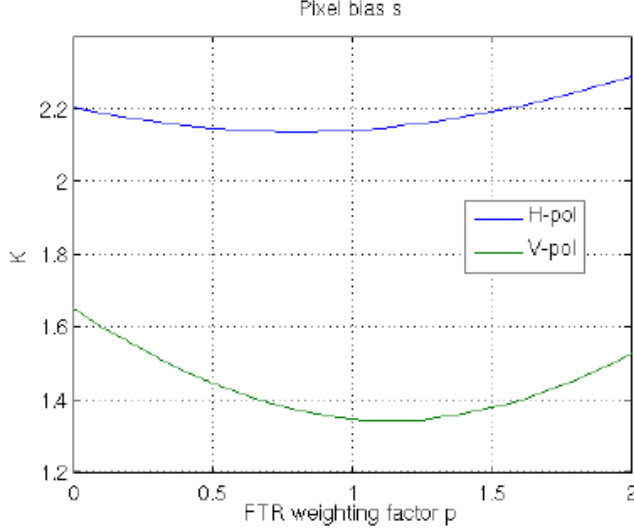


Fig. 3. Pixel bias wrt FTR weighting parameter.

Let's consider the modified FTT equation where a weighting parameter p is introduced to the scaling factor of the FTR:

$$V'_{kj} = V_{kj} - p(T_A - T_R)FTR(k, j) \quad (2)$$

where V'_{kj} is the transformed visibility between receiver k and j , V_{kj} is the measured visibility, T_A is the average scene brightness temperature and T_R is the receiver's physical temperature.

According to Corbella's visibility function, the minimum error in the brightness temperature, the so-called pixel bias, is achieved when the FTT is applied with the weighting parameter p set to 1. As T_A is the average of the antenna temperature in Horizontal (H) and Vertical (V) polarization, the FTT optimum is in the midpoint between the optimum of H and V polarization.

The experimental minimization of the pixel bias of the measured brightness temperature with respect to the reference simulated scene is achieved when p is 1. Fig. 3 shows that $p = 1$ is the midpoint between the optimum of H and V polarization as Corbella's visibility function predicted.

3.3. Comparison between anechoic chamber and cold sky measurements

SMOS measurements have been compared to several simulated visibilities (Fig. 4). On one hand, the cold sky measurements are smaller than expected by Corbella's visibility function, but larger than the ones predicted by the classic radioastronomy equation and even larger than the measurements obtained in the anechoic chamber at ESTEC.

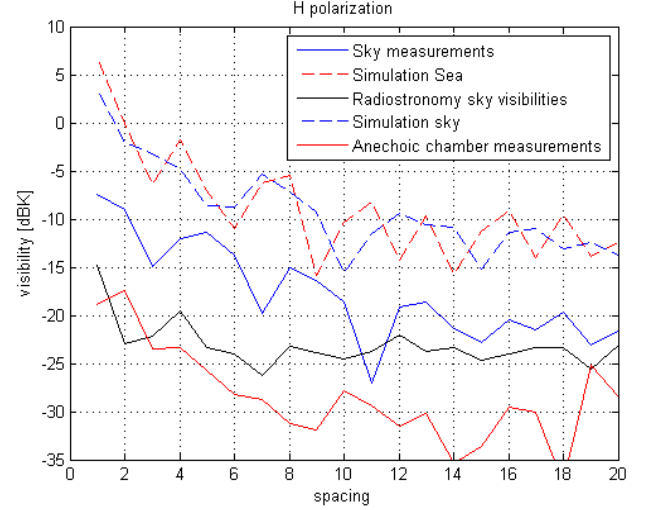


Fig. 4. Comparison between measurements and simulations for H-pol.

The partial discrepancy between the cold sky measurements and the predicted visibilities could be attributed to an underestimation of contributors like the antennas' backlobes and the Sun contribution in the simulation. The impact of these contributors is currently under analysis.

On the other hand, the visibility simulation over an ocean scenario, with the same geometry of SMOS, produces also large visibilities. That contradicts the intuition based on the relationship between visibility magnitude and contrast between scene brightness temperature and instrument physical temperature. According to those simulations, that relationship is only valid for flat targets. However, on scenes with discontinuities several frequencies are excited and the prediction of the value of the visibilities is not evident. This is the case of the nominal measurements of SMOS where the Earth horizon is in the field of view. In other words, SMOS visibilities measured looking downwards are not necessary smaller than the cold sky visibilities.

4. CONCLUSIONS

The Corbella's visibility function has been experimentally validated with HUT-2D and in-orbit SMOS data.

The comparison between the HUT-2D normalized visibilities for different targets has been presented. The gradual increase with the contrast between the brightness temperature scene and the receivers' physical temperature follows the Corbella's predicted behaviour.

On the other hand, the validation of the Corbella's visibility function using in-orbit SMOS data has been presented for the first time. The overall results of three

different commissioning activities conducted to validate the Corbella's visibility function, and therefore the MIRAS instrument model, are positive. However, the impact of the antennas' backlobes and Sun contribution are currently under analysis due to the partial discrepancy observed between cold sky measurements and the simulated visibilities.

5. REFERENCES

[1] Y. Kerr, P. Waldteufel, J. Wigneron, J. Martinuzzi, J. Font, and M. Berger, "Soil Moisture Retrieval from Space: The Soil Moisture and Ocean Salinity (SMOS) Mission," *IEEE Trans. Geosci. Remote Sensing*, vol. 39, no. 8, pp. 1729–1735, Aug. 2001

[2] J. Font, G. S. E. Lagerloef, D. M. Le Vine, A. Camps, and O. Zanifé, "The Determination of Surface Salinity With the European SMOS Space Mission," *IEEE Trans. Geosci. Remote Sensing*, vol. 42, no. 10, pp. 2196–2205, Oct. 2004.

[3] K. D. McMullan, M. A. Brown, M. Martín-Neira, W. Rits, S. Ekholm, J. Marti, and J. Lemanczyk, "SMOS: The Payload," *IEEE Trans. Geosci. Remote Sensing*, vol. 46, no. 3, pp. 594–605, Mar. 2008

[4] C. S. Ruf, C. T. Swift, A. B. Tanner, and D. M. Le Vine, "Interferometric synthetic aperture microwave radiometry for the remote sensing of the Earth," *IEEE Trans. Geosci. Remote Sensing*, vol. 26, no. 5, pp. 597–611, Sept. 1988.

[5] A. J. Camps, "Application of interferometric radiometry to Earth observation," Ph.D. dissertation, Univ. Catalonia, Barcelona, Spain, Nov. 1996

[6] I. Corbella, N. Duffo, M. Vall-llossera, A. Camps, and F. Torres, "The Visibility Function in Interferometric Aperture Synthesis Radiometry," *IEEE Trans. Geosci. Remote Sensing*, vol. 42, no. 8, pp. 1677–1682, Aug. 2004.

[7] M. Martín-Neira, I. Cabeza, C. Perez, M. A. Palacios, M. A. Guijarro, S. Ribo, I. Corbella, S. Blanch, F. Torres, N. Duffo, V. Gonzalez, S. Beraza, A. Camps, M. Vall-llossera, S. Tauriainen, J. Pihlflyckt, J. P. Gonzalez, and F. Martín-Portuerras, "AMIRAS—An airborne MIRAS demonstrator," *IEEE Trans. Geosci. Remote Sens.*, vol. 46, no. 3, pp. 705–716, Mar. 2008.

[8] K. Rautiainen, J. Kainulainen, T. Auer, J. Pihlflyckt, J. Kettunen, and M. T. Hallikainen, "Helsinki University of Technology L-band airborne synthetic aperture radiometer," *IEEE Trans. Geosci. Remote Sens.*, vol. 46, no. 3, pp. 717–726, Mar. 2008

[9] P. Moreno-Galbis, J. Kainulainen, and M. Martín-Neira, "Experimental Demonstration of the Corbella Equation for Aperture Synthesis Microwave Radiometry," *IEEE Trans. Geosci. Remote Sens.*, vol. 45, no. 4, pp. 945–957, Apr. 2007

[10] M. Martín-Neira, M. Suess, J. Kainulainen, and F. Martín-Portuerras, "The Flat Target Transformation," *IEEE Trans. Geosci. Remote Sens.*, vol. 46, no. 3, pp. 613–620, Mar. 2008.